Journal of Membrane Science 685 (2023) 121955

Contents lists available at ScienceDirect

Journal of Membrane Science

journal homepage: www.elsevier.com/locate/memsci

A mathematical model for initial design iterations and feasibility studies of oxygen membrane reactors by minimizing Gibbs free energy

Kai Bittner [a,b,*], Nikolaos Margaritis [a], Falk Schulze-Küppers [a], Jörg Wolters [a], Ghaleb Natour [a,c]

[a] Central Institute of Engineering, Electronics and Analytics (ZEA), Forschungszentrum Jülich GmbH, Jülich, Germany
[b] Faculty of Mechanical Engineering, RWTH Aachen University, Aachen, Germany
[c] ISF, Faculty of Mechanical Engineering, RWTH Aachen University, Aachen, Germany

ARTICLE INFO

Keywords:
Membrane reactor
Water splitting
Partial oxidation
Oxygen permeable membrane
Reactor modelling

ABSTRACT

Ceramic Membrane Reactors offer an opportunity towards the transition to renewable energies and defossilized economies by efficiently coupling chemical reactions and heat utilization. To identify viable processes, mathematical models are needed that allow a straightforward assessment. In this study, a generalized model is presented that can be applied to membrane reactor concepts using a mixed oxygen transport membrane. The model assumes chemical equilibrium which is realized by minimizing the Gibbs free energy in the individual reaction chambers. Both reaction chambers are coupled by the Wagner equation to account for the oxygen ion flux through the membrane. Experimental data from the literature were used to validate the model for water splitting, partial oxidation of methane, and the coupling of these two processes. The model allows to investigate various process parameters such as oxygen flux and gas compositions, making the model particularly suitable for feasibility studies and initial design iterations for new reactor developments.

1. Introduction

The implementation of oxygen membranes into reactors opens up new possibilities for chemical processes, but it also poses new challenges regarding the mathematical modelling of these processes. First computational fluid dynamics (CFD) models have been developed modelling the reactions on the membrane surface using rate equations [1–4]. The oxygen partial pressure in this case is a function of the reaction rates. While this may be the most accurate approach it relies on a fitting to experimental data as the reaction kinetics on the surface of a membrane are usually not known and depend on the catalytic activity of the membrane. In particular, the water splitting reaction was not modelled, but a mixture of hydrogen and oxygen was used instead [2,4].

Besides using reaction rates, the oxygen partial pressure may also be estimated from the chemical equilibrium. This has been done in previous works by calculating the chemical equilibrium for the assumed reaction to determine the thermodynamic limit of a specific membrane reactor concept [5,6]. While this approach does not take into account possible limitations of the reactor performance due to slow reaction kinetics as the reactions are assumed to be infinitely fast, it simplifies the mathematical modelling. The equilibrium constant depends on the temperature only [7] and therefore requires no fitting to experimental data. The assumption of infinitely fast reactions is followed within this work by calculating the gas components and oxygen partial pressure on both sides of the membrane using the Gibbs free energy minimization method (non-stoichiometric approach). The advantage of this method is that no stoichiometric equations have to be set up and the model can therefore be theoretically applied to any gas mixture without modifying it. It was in previous studies for example applied to steam reforming, partial oxidation and gasification processes [8–13]. This approach is then coupled with a transport equation for the oxygen ion flux through the membrane and the resulting effect on the gas components and oxygen partial pressure. For this purpose, the Wagner equation is used, applicable to materials consisting of ion and electronic conductors (e.g. mixed ionic-electronic conducting membranes) if the ambipolar conductivity is known. For dual phase membranes, this value can be estimated in a first approximation from the proportions of the electron conducting and ion conducting phases, as well as their partial conductivities. Furthermore, geometrical factors such as the tortuosity of the phases should be taken into account. Such a model was developed for ceramic-carbonate dual-phase membranes by Rui et al. [14].

The input parameters of the model are temperature, operating pressure, flow rates, inlet gas compositions, membrane area, membrane thickness and ambipolar conductivity of the membrane. It allows to estimate various process parameters helpful for designing experiments

* Corresponding author at: Central Institute of Engineering, Electronics and Analytics (ZEA), Forschungszentrum Jülich GmbH, Jülich, Germany.
E-mail address: k.bittner@fz-juelich.de (K. Bittner).

https://doi.org/10.1016/j.memsci.2023.121955
Received 16 June 2023; Received in revised form 18 July 2023; Accepted 21 July 2023
Available online 24 July 2023

(provided the ambipolar conductivity of the material is known beforehand) such as the oxygen partial pressure in both reaction chambers, the resulting oxygen transport through the membrane, outlet flow rates and outlet gas compositions. The model is validated against experimental data from the literature for three frequently studied membrane reactor configurations. For this purpose, a range of ambipolar conductivity of the membranes used in the respective experiments was estimated from material data in the literature and used as an input parameter in addition to given experimental parameters.

2. Modelling approach

The model presented here refers to a continuous reactor in which two reaction chambers are separated by an oxygen membrane. The assumptions made are similar to the assumptions made by Akin et al. [5]. These are:

- Constant temperature, constant pressure, ideal gases
- Perfect mixing i.e. the composition of the effluent gases is equal to the gas composition on the membrane
- Infinitely fast reactions, i.e. reactions are assumed to be in state of equilibrium

Due to these assumptions there are some limitations to the model. Since perfect mixing is assumed and the driving force for oxygen permeation is therefore calculated from the effluent gas compositions, the membrane geometry and configuration is not considered explicitly. This allows for a generalized modelling. However, it should be noted here that the partial pressure of oxygen at the outlet of the membrane reactor may differ from the partial pressure of oxygen at the membrane surface. This difference could potentially lead to a discrepancy between the predicted oxygen flux and the actual measured data. For example, concentration polarization at the membrane surface may cause the driving force for oxygen permeation to be overestimated by the model. On the other hand, the series connection of several membranes or the utilization of a long tubular membrane may result in an underestimation. This is because the driving force decreases in flow direction and is calculated from the outlet conditions by the model.

The assumption of chemical equilibrium allows to model new reactor concepts without requiring an extensive study of the reaction mechanism and provides insight into the thermodynamic limits. Dependent on the reaction rates and residence time, the gas mixture at the reactor outlet may not be in chemical equilibrium which for example can lead to an overestimation of CO species and underestimation of CO_2 species [10,11,13]. In addition, since this study examines membrane reactors in which oxygen permeation depends on oxygen partial pressure, it should be noted that this may lead to an overestimation of the oxygen flux if it is limited by the rates of oxygen-releasing and oxygen-consuming reactions.

For the calculation of the equilibrium state, the Gibbs free energy minimization approach is used in this work. This approach makes use of the property that a mixture at constant temperature and constant pressure is in chemical equilibrium when the Gibbs free energy reaches its minimum [15]. The total Gibbs free energy can be written as the sum of the Gibbs free energies of all species i,

$$G = \sum_i N_i G_{m,i}, \tag{1}$$

where $G_{m,i}$ is the molar Gibbs free energy and N_i is the number of moles of species i. For a mixture of ideal gases, the partial pressure dependency can be expressed as

$$G = \sum_i N_i \left(G^0_{m,i}(T) + RT \ln \frac{p_i}{P^0} \right), \tag{2}$$

where $G^0_{m,i}(T)$ is the molar Gibbs free energy at standard state pressure, R is the universal gas constant, T is the temperature, p_i is the partial pressure and P^0 is the standard state pressure. The partial pressure is related to the static pressure P as

$$p_i = \frac{N_i}{\sum_i N_i} P. \tag{3}$$

In order to find a physical feasible solution for the minimization of Eq. (2), constraints must be added. Firstly, the number of atoms in the mixture in its equilibrium state must be equal to the number of atoms in its initial state. Furthermore, the number of moles cannot be negative. For the minimization problem, the molar Gibbs energy at standard state pressure may further be replaced by the Gibbs energy of formation at standard state pressure ΔG^0, which can be taken from thermodynamic property tables [16]. Given that and substituting Eq. (3), the chemical equilibrium of a mixture at constant temperature and pressure can be found by solving a constrained minimization problem in the form:

$$\begin{aligned} \min_{\boldsymbol{N}} \quad & f = \sum_i N_i \left(\frac{\Delta G^0(T)}{RT} + \ln \frac{P}{P^0} + \ln \frac{N_i}{\sum_j N_j} \right) \\ \text{s.t.} \quad & \sum_i \boldsymbol{a_i}(N_i - N_{i,0}) = \boldsymbol{0} \\ & \boldsymbol{N} \geq \boldsymbol{0} \end{aligned} \tag{4}$$

$\boldsymbol{a_i}$ is a vector with length of the number of occurring atom types, that contains the number of the respective atom of one molecule of species i in its row and $N_{i,0}$ is the number of moles in the initial state.

Since the use of a membrane leads to oxygen transport from the side with high oxygen partial pressure to the side with low oxygen partial pressure, the oxygen flux through the membrane will influence the equilibrium state. Therefore it has to be included into the model. For this purpose, the simplified Wagner equation was used to couple the two gas compartments. Here oxygen transport through the crystal lattice is assumed to be the rate-determining step [17]. However, for very thin membranes with high oxygen transport rate, it may be reasonable to also consider the surface exchange reactions, for example by including a characteristic length [18] or replacing the Wagner equation by the Xu-Thomson model [19]. Another factor not taken into account here is the performance reduction observed with asymmetric membranes, due to concentration polarization in the porous region [20]. This effect has been modelled for oxygen membrane modules with inert gases in previous studies by including the binary friction model to calculate the oxygen partial pressure in the porous region [21,22]. A similar approach may also be used to extend the model presented here, e.g. by distinguishing between the gas composition in the porous region and the gas composition at the outlet of the reactor. However, further experiments would be needed for validation.

Due to the oxygen partial pressure dependence of the ambipolar conductivity and the different partial pressures on both sides of the membrane, an average ambipolar conductivity is assumed. For well-studied materials, the ambipolar conductivity can also be modelled as a function of partial pressure, but this was not done here due to the limited data available. For the sake of convention, oxygen flux is referred to oxygen molecules O_2 and molecular oxygen partial pressure here. The oxygen flux in mol m^{-2} s^{-1} can then be modelled by the Wagner equation as

$$j_{O_2} = \frac{RT\overline{\sigma}_{amb}}{16F^2L} \ln \frac{p_{O_2,f}}{p_{O_2,s}} \tag{5}$$

where $p_{O_2,f}$ and $p_{O_2,s}$ denotes the oxygen partial pressure on the feed and sweep side, respectively, $\overline{\sigma}_{amb}$ is the average ambipolar conductivity (material parameter), F is the Faraday constant and L is the thickness of the membrane. Inserting Eq. (3), the Wagner Equation can be transformed into

$$j_{O_2} = \frac{RT\overline{\sigma}_{amb}}{16F^2L} \left(\ln \frac{N_{O_2,f}}{N_{O_2,s}} + \ln \frac{\sum_i N_{i,s}}{\sum_i N_{i,f}} + \ln \frac{P_f}{P_s} \right), \tag{6}$$

where the index f denotes the feed and the index s denotes the sweep side.

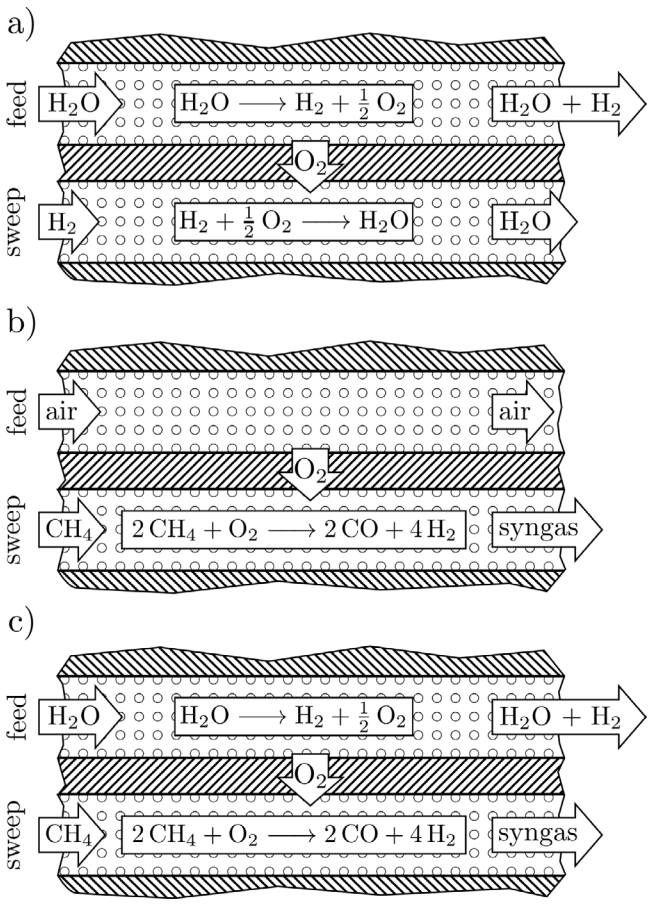

Fig. 1. Validated reactor concepts.

Given an expression for the oxygen flux through the membrane, the Gibbs energy minimization problem introduced in Eq. (4) can now be extended to be applicable for an oxygen membrane reactor. As in the general case the oxygen can be involved into reactions on both sides of the membrane, the Gibbs free energy needs to be minimized on the feed as well as the sweep side. Furthermore, as continuously gas flows are considered here, we replace the number of moles N_i by the molar flow rate $\dot{N}_i$. Including the oxygen flux into the atomic balance the complete model then reads:

$$\begin{aligned} \min_{\dot{\boldsymbol{N}}_{f/s}} \quad & f_{f/s} = \sum_i \dot{N}_{i,f/s} \left(\frac{\Delta G^0(T)}{RT} + \ln \frac{P_{f/s}}{P^0} + \ln \frac{\dot{N}_{i,f/s}}{\sum_j \dot{N}_{j,f/s}} \right) \\ \text{s.t.} \quad & \sum_i \boldsymbol{a_i} (\dot{N}_{i,f/s} - \dot{N}_{i,f/s,0}) \pm \boldsymbol{j} A_{mem} = \boldsymbol{0} \\ & \dot{\boldsymbol{N}}_{f/s} \geq \boldsymbol{0} \end{aligned} \tag{7}$$

$$\text{with} \quad j_k = \begin{cases} 2 j_{O_2}, & k = O \\ 0, & k \neq O \end{cases}$$

$$j_{O_2} = \frac{RT \overline{\sigma}_{amb}}{16 F^2 L} \left(\ln \frac{\dot{N}_{O_2,f}}{\dot{N}_{O_2,s}} + \ln \frac{\sum_i \dot{N}_{i,s}}{\sum_i \dot{N}_{i,f}} + \ln \frac{P_f}{P_s} \right)$$

The term $\pm \boldsymbol{j} A_{mem}$ which is negative on the feed side and positive on the sweep side includes the oxygen flux through the membrane into the atomic balance. For this study, the problem was solved using *Cantera* [23] coupled with the root finding algorithm from *SciPy* [24] in order to find the oxygen flux that satisfies the Wagner equation in the equilibrium state. The thermodynamic data was taken from *Gri Mec 3.0* [25], which includes 53 species. The model can be extended to include further species by inserting additional thermodynamic data (e.g., from the NASA polynomial database [26]).

3. Validation of the proposed model

The introduced model was validated against experimental data taken from the literature [27–29] for three different frequently studied membrane reactor configurations.

3.1. Validated concepts and general approach

The considered configurations are shown in Fig. 1 and are briefly described below. Furthermore the assumed main reactions are also briefly discussed in order to explain deviations from experimental data to our model.

The first configuration used to validate the model is the thermal decomposition of water vapour on the feed side using hydrogen as the reducing gas on the sweep side (cf. Fig. 1 a)). Since two hydrogen molecules remain for every oxygen molecule removed from the feed side, the production rate of hydrogen generation can be expressed as

$$\text{H}_2 \text{ rate} = 2 j_{O_2}. \tag{8}$$

On the sweep side, the oxygen is consumed by the hydrogen. This is required to produce reasonable amounts of hydrogen on the feed side as the oxygen partial pressure in the steam is very low (in the order of 0.1–1 Pa between 900–1000 °C according to chemical equilibrium [23, 25]). While this concept does not yield to a net hydrogen production, it can be used to produce high purity hydrogen on the feed side by consuming a low purity hydrogen mixture on the sweep side [30].

The second concept, shown in Fig. 1 b), is the partial oxidation of methane (POM) using air as feed gas. In this case, the membrane is used to feed pure oxygen from air to methane in order to produce synthesis gas. The oxygen is therefore not involved into any relevant reaction with another species on the feed side. The POM reaction mechanism is still not completely understood, and involves several different reaction paths including a combustion of CH_4 and reforming reactions of H_2O and CO_2 [31,32]. To quantify how much of the reacting methane is converted to CO, the

$$\text{CO selectivity} = \frac{\dot{N}_{CO}}{\dot{N}_{CH_4,0} - \dot{N}_{CH_4}} \tag{9}$$

is used here. Usually a catalyst is used to increase the CO selectivity [33]. The stoichiometry of the partial oxidation shows that a H_2/CO ratio of about 2:1 is reachable. Besides the exothermic nature of the process, this may be one reason to use the POM as an alternative to steam reforming, as a different H_2/CO ratio in the synthesis gas can be reached (3:1 for steam reforming) [32,34].

The last concept considered here, shown in Fig. 1 c), is a combination of water splitting and POM. For this purpose, methane is used as the reducing gas on the sweep side, while steam is used on the feed side. The process thus delivers both pure hydrogen and synthesis gas as valuable products [35].

The experimental data for water splitting using hydrogen as sweep gas (Fig. 1 a)), the POM using air as feed gas (Fig. 1 b)) and the water splitting using methane as sweep gas (Fig. 1 c)) were taken from Cai et al. [27], Kozhevnikov et al. [29] and Zhang et al. [28], respectively. Apart from the ambipolar conductivity of the membrane, all necessary parameters for the model are given in the experiments. A range for this parameter, denoted as $\overline{\sigma}_{amb,lit}$, was therefore estimated for the respective membrane materials using literature data [27,36,37]. This is to show that the model can be used to estimate the performance of processes without the need for experiments, provided that the ambipolar conductivity is known. Since the estimates of the ambipolar conductivity are rather rough, the model was further fitted by varying its value in order to show the impact on the results. The fitted value is denoted as $\sigma_{amb,fit}$. Further information on this estimation can be found in Appendix B.

For the sake of convention, the molar flow rates were converted to volumetric flow rates according to the ideal gas law by setting the temperature equal to the reference temperature for the flow rates used in the respective experiments. A summary of the model input data is provided in Appendix A.

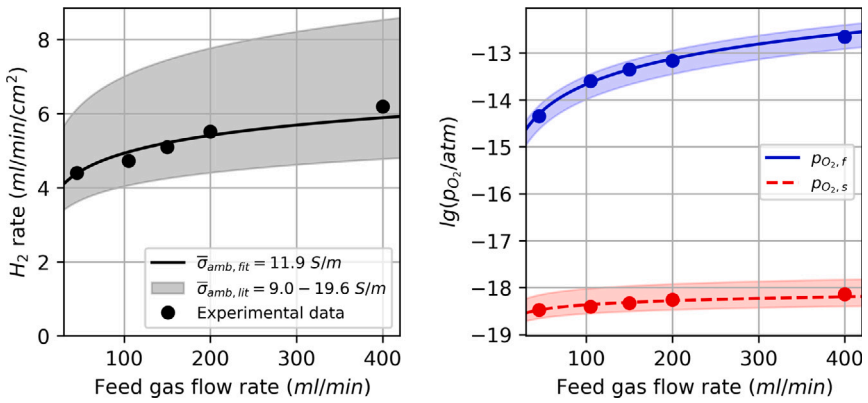

Fig. 2. Comparison of the model to experimental data (dots) [27] for the concept of water splitting using hydrogen as sweep gas. The shaded areas refer to the results using a range for $\bar{\sigma}_{amb}$ estimated from the literature [27] (cf. Appendix B). The lines refer to the results using a fitted value for $\bar{\sigma}_{amb}$. The sweep gas flow rate was kept constant at 100 ml/min with a H_2 concentration of 50%.

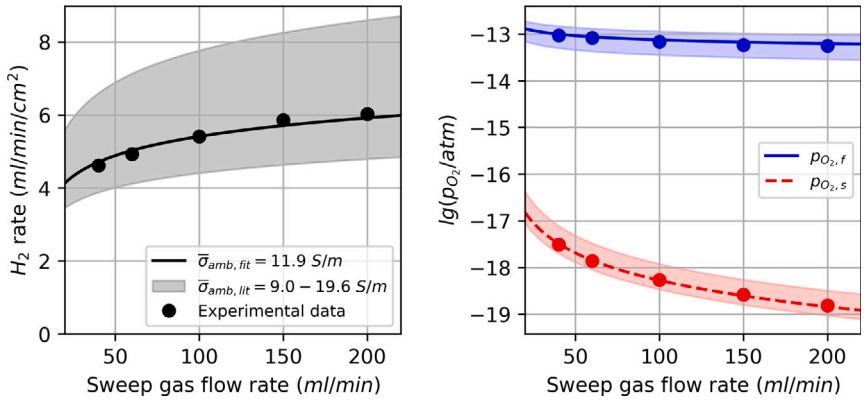

Fig. 3. Comparison of the model to experimental data (dots) [27] for the concept of water splitting using hydrogen as sweep gas. The shaded areas refer to the results using a range for $\bar{\sigma}_{amb}$ estimated from the literature [27] (cf. Appendix B). The lines refer to the results using a fitted value for $\bar{\sigma}_{amb}$. The feed gas flow rate was kept constant at 200 ml/min and the H_2 concentration in the sweep gas was kept at 50%.

3.2. Water splitting using hydrogen as sweep gas

Experimental data taken from Cai et al. [27] were used to validate the model for the concept of water splitting using hydrogen as sweep gas. A planar dual-phase membrane with a thickness of 500 μm and an active membrane area of 0.85 cm^2 was used in the experiments. The hydrogen production rate given by Eq. (8) and the oxygen partial pressure given by Eq. (3) were computed by the model and compared with the experimental data. Except for the feed gas flow rate, the sweep gas flow rate and the H_2 concentration in the sweep gas, all model input parameters were kept constant (cf. Appendix A).

The impact of the feed gas flow rate, the sweep gas flow rate and the H_2 concentration in the sweep gas on the results is shown in Fig. 2, Fig. 3 and Fig. 4, respectively. The model is in good agreement with the experimental data for both, the hydrogen production rate as well as the oxygen partial pressure. This indicates that the water splitting reaction and the hydrogen combustion on the membrane surface can be modelled with a good approximation by assuming chemical equilibrium under the operating conditions for the used catalyst, which is a porous Ni/Sm-doped ceria layer on the membrane surface. The results further show the importance of measuring the ambipolar conductivity as accurately as possible to estimate the reactor performance, as the range given in the literature results in a wide range of reachable hydrogen production rates.

3.3. Partial oxidation of methane using air as feed gas

Experimental data taken from Kozhevnikov et al. [29] were used to validate the model for the concept of POM using air as the feed gas. A planar membrane with a thickness of 1900 μm and an active area of 1.6 cm^2 was used in the experiments. The oxygen flux through the membrane, the methane consumption and the CO selectivity calculated by Eq. (9) were compared to the experimental data. Except for the sweep gas flow rate, all model input parameters were kept constant (cf. Appendix A). On the feed side, a constant oxygen partial pressure of 0.21 atm was assumed, as the feed flow rate is unknown.

The impact of the sweep gas flow rate on the results is shown in Fig. 5. The model shows good agreement for the course of the evaluated data when the ambipolar conductivity is fitted. When using the literature values for the conductivity, the oxygen flux is overestimated which may be explained by the results obtained by Serra et al. [38]: The final steps of the oxygen permeation process involve the desorption and reaction of oxygen ions and molecules at surface active sites on the sweep gas side. However, a part of the required active sites is occupied/blocked by CO_2 species. As a result, CO_2 adsorption leads to a reduction in the active sites available for the exchange reactions. This effect is not represented by the simulation and results in an overestimation of the oxygen flux by a factor of 1.5 at 900 °C, as observed by Serra et al. [38]. Another deviation between experimental and simulated data is shown in the methane conversion at the highest considered sweep flow rate. This indicates that the CH_4 conversion may get overestimated for high sweep gas flow rates.

3.4. Water splitting using methane as sweep gas

Experimental data taken from Zhang et al. [28] were used to validate the model for the concept of water splitting using methane

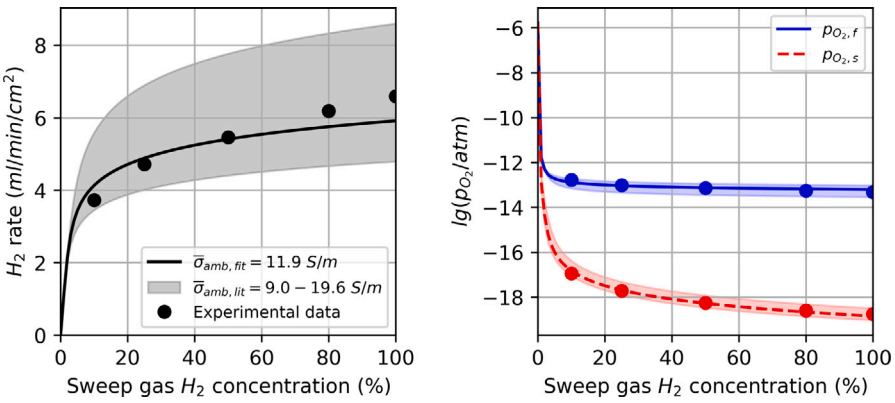

Fig. 4. Comparison of the model to experimental data (dots) [27] for the concept of water splitting using hydrogen as sweep gas. The shaded areas refer to the results using a range for $\bar{\sigma}_{amb}$ estimated from the literature [27] (cf. Appendix B). The lines refer to the results using a fitted value for $\bar{\sigma}_{amb}$. The feed and sweep gas flow rates were kept constant at 100 ml/min and 200 ml/min, respectively.

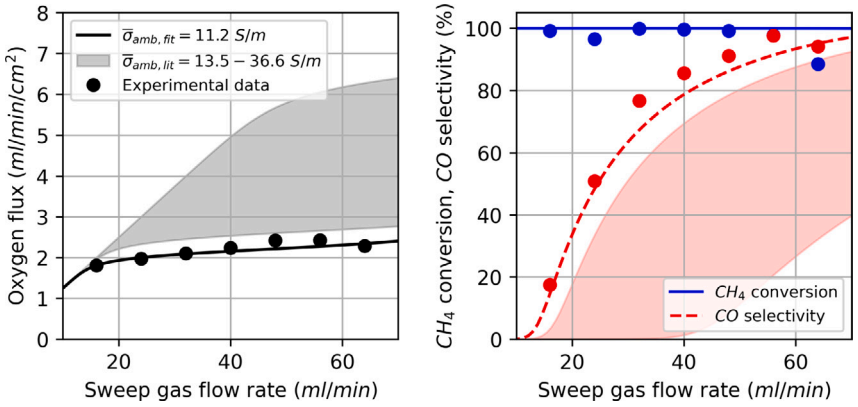

Fig. 5. Comparison of the model to experimental data [29] for the concept of POM using air as feed gas. The shaded areas refer to the results using a range for $\bar{\sigma}_{amb}$ estimated from the literature [36] (cf. Appendix B). The lines refer to the results using a fitted value for $\bar{\sigma}_{amb}$.

as sweep gas. A hollow fibre membrane with a length of 5 cm, an inner diameter of 1.3 mm, an outer diameter of 1.8 mm and an active membrane area of 2.41 cm^2 was used in the experiments. The hydrogen production rate given by Eq. (8), the methane consumption and the CO selectivity calculated by Eq. (9) were computed using the model and compared to the experimental data. Besides the feed gas flow rate, the sweep gas flow rate and the H_2O concentration in the feed gas, all model input parameters were kept constant (cf. Appendix A).

The impact of the feed gas flow rate and the sweep gas flow rate on the results is shown in Fig. 6 and Fig. 7, respectively. The principal course of the experimental obtained values is well represented by the model, but using the extrapolated range for the ambipolar conductivity from the literature the H_2 rate is overestimated. However, this overestimation may be explained by uncertainties regarding the extrapolation by the Arrhenius fit (cf. Appendix B) for which the assumed temperature dependency may change significantly at higher temperatures. The CH_4 conversion and the CO selectivity tend to get overestimated by the model even if the fitted value is used. This is in agreement with previous studies which showed that the assumption of chemical equilibrium tends to overestimate the production of CO species and underestimate the production of CO_2 species [10,11,13]. The achievable CO selectivity and CH_4 conversion thus strongly depend on the catalyst and only a tendency can be predicted by the model.

4. Conclusion

A generalized model for the estimation of the performance of oxygen membrane reactors was proposed and validated against experimental data from the literature for three different frequently studied concepts. The model is able to approximately predict the oxygen flux through the membrane before performing the experiments if the ambipolar conductivity of the material is known, which can be estimated, for example, from literature data, as is done in this work. Values for the expected deviations cannot be given here because the results depend strongly on the accuracy of the estimation of the ambipolar conductivity, but the values were always in the same order of magnitude as the data from the experiments. Due to the implemented non stoichiometric equilibrium approach, the model allows to quickly generate data for arbitrary oxygen membrane reactor processes without requiring knowledge of the reaction mechanism. However, the formation of the species involved into reactions, that are rather slow compared to the oxidation reactions, such as CO in the POM process, can only be predicted by tendency and the reactor performance may be overpredicted if it is limited by reaction rates. Other limitations are that the flow characteristics such as the pressure/temperature field and the influence of geometry cannot be studied with the proposed model.

From the features and limitations of the model, the possible applications can be derived. It is applicable for feasibility studies and first design iterations for new reactor concepts as well as for sensitivity studies on certain parameters like pressure, temperature, flow rates and the ratio of certain gases on the feed and sweep side of the membrane. Its main strength is the fast and simple algorithm that does not need huge computational resources. However, it should be kept in mind that it cannot replace a detailed design of a membrane reactor for more complex processes and flow fields.

In future studies the influence of other factors not taken into account in here, such as diffusion processes in the gas phase, reaction rates and the porous support in asymmetric membranes should be investigated.

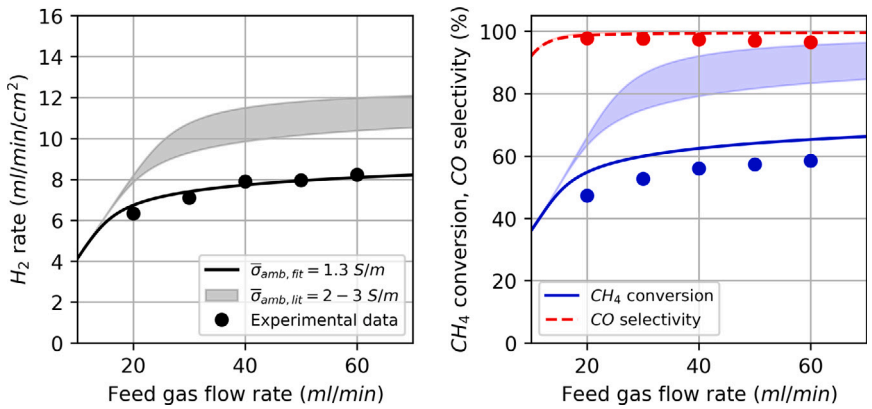

Fig. 6. Comparison of the model to experimental data [28] for the concept of water splitting using methane as sweep gas. The shaded areas refer to the results using a range for $\bar{\sigma}_{amb}$ estimated from the literature [37] (cf. Appendix B). The lines refer to the results using a fitted value for $\bar{\sigma}_{amb}$. The H_2O concentration in the feed gas was kept constant at 100% and the sweep gas flow rate was kept at 30 ml/min.

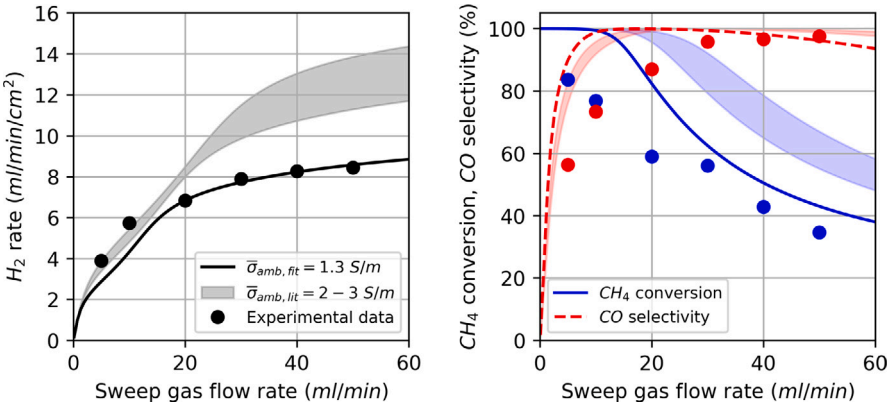

Fig. 7. Comparison of the model to experimental data [28] for the concept of water splitting using methane as sweep gas. The shaded areas refer to the results using a range for $\bar{\sigma}_{amb}$ estimated from the literature [37] (cf. Appendix B). The lines refer to the results using a fitted value for $\bar{\sigma}_{amb}$. The feed gas flow rate was kept constant at 50 ml/min with a H_2O concentration of 80%.

To study the effects of diffusion processes in the gas phase, as a next step it is planned to implement the Wagner equation and chemical equilibrium calculation of the oxidation reactions at the surface of the membrane into a CFD model. This approach will provide insight into the geometric effects on oxygen partial pressure at the membrane surface and resulting potential deviations in predicted reactor performance from the model presented here. It is furthermore planned to conduct experiments using an oxygen membrane reactor with multiple membranes to validate the applicability of the model to industrial scale reactors. Finally, for promising processes, membrane materials and catalysts, the reaction kinetics at the membrane surface should be investigated experimentally to develop specifically tailored models. This would allow a detailed investigation of these concepts that go beyond initial design iterations and feasibility studies.

CRediT authorship contribution statement

Kai Bittner: Conceptualization, Methodology, Software, Validation, Formal analysis, Investigation, Writing – original draft, Writing – review & editing, Visualization. **Nikolaos Margaritis:** Writing – review & editing, Project administration. **Falk Schulze-Küppers:** Validation, Investigation, Writing – review & editing. **Jörg Wolters:** Resources, Writing – review & editing, Supervision. **Ghaleb Natour:** Writing – review & editing, Supervision.

Declaration of competing interest

The authors declare that they have no known competing financial interests or personal relationships that could have appeared to influence the work reported in this paper.

Data availability

The data that has been used is confidential

Acknowledgments

This work was supported by the Federal Ministry of Education and Research (Germany) [grant 03SF0648].

Appendix A. Model input data

The model input data used for the validation are summarized in Table A.1. H_2O–H_2 denotes water splitting using hydrogen as sweep gas, O_2–CH_4 denotes POM using air as feed gas and H_2O–CH_4 denotes water splitting using methane as sweep gas. T_{ref} is the temperature the flow rates refer to according to the ideal gas law. $X_{i,f,0}$ and $X_{i,s,0}$ denote the molar fraction of the reacting species in the initial mixture of the feed and sweep side, respectively.

Table A.1
Summary of the model input data based on literature values [27–29,36,37].

		H_2O–H_2	O_2–CH_4	H_2O–CH_4
T	(°C)	900	900	950
P_f	(atm)	1	1	1
P_s	(atm)	1	1	1
T_{ref}	(°C)	25	25	950
Q_f	(ml/min)	30–420	$\rightarrow \infty$	10–70
$X_{i,f,0}$	(%)	90	21	80–100
Q_s	(ml/min)	20–220	0–80	0–55
$X_{i,s,0}$	(%)	0–100	10	100
A_{mem}	(cm^2)	0.85	1.60	2.41
$\sigma_{amb,lit}$	(S/m)	9.0–19.6	13.5–36.5	2–3
$\sigma_{amb,fit}$	(S/m)	11.9	11.2	1.3
L	(μm)	500	1900	250

Appendix B. Estimation of the ambipolar conductivities

B.1. SDC-SFM dual-phase membrane

For the experiments on water splitting using hydrogen as sweep gas, Cai et al. [27] used a dual-phase membrane consisting of 70 wt % $Ce_{0.85}Sm_{0.15}O_{1.925}$ and 30 wt % $Sr_2Fe_{1.5}Mo_{0.5}O_{6-\delta}$ (SDC-SFM). At 900 °C, a range of about 10–20 S/m was given for the ionic conductivity σ_i and a range of 96–944 S/m for the total conductivity σ_t. The resulting estimated range for the average ambipolar conductivity calculated from the ionic and electronic conductivity contribution as

$$\sigma_{amb} = \frac{\sigma_i \sigma_e}{\sigma_i + \sigma_e} = \frac{\sigma_i(\sigma_t - \sigma_i)}{\sigma_t} \tag{B.1}$$

is 9.0–19.6 S/m.

B.2. LSF membrane

For the experiments on POM using air as feed gas, Kozhevnikov et al. [29] used a $La_{0.5}Sr_{0.5}FeO_{3-\delta}$ (LSF) membrane. This material has been studied by Patrakeev et al. [36], who fitted an expression of the form

$$\sigma_t = \sigma_i + \sigma_n^\circ \left(\frac{p_{O_2}}{\text{atm}}\right)^{-1/4} + \sigma_p^\circ \left(\frac{p_{O_2}}{\text{atm}}\right)^{1/4}, \tag{B.2}$$

where σ_n° and σ_p° represent the n- and p-type contributions to the electronic conductivity. The fitted values at 900 °C are σ_i = 36.6 S/m, σ_n° = 0.00561 S/m and σ_p° = 20200 S/m. The electronic conductivity reaches its minimum at about $p_{O_2} = 10^{-13}$ atm. By inserting Eq. (B.2) into Eq. (B.1), a corresponding minimum ambipolar conductivity of 13.5 S/m is obtained. The maximum reachable ambipolar conductivity for $\sigma_e >> \sigma_i$ is σ_i. The range for the average ambipolar conductivity is therefore given by these bounds.

B.3. LCF membrane

For the experiments on water splitting using methane as sweep gas, Zhang et al. [28] used a $La_{0.8}Ca_{0.2}Fe_{0.94}O_{3-\delta}$ (LCF) membrane. This material has been studied by Bidrawn et al. [37] who investigated the ionic conductivity in a temperature range of 650–800 °C. For the estimate, the experimental values were extrapolated to the operating temperature of 950 °C by assuming an Arrhenius behaviour as shown in Fig. B.8. The resulting ionic conductivity is between 2 S/m and 3 S/m. As the impact of the oxygen partial pressure on the electronic conductivity is unknown, $\sigma_e >> \sigma_i$ is assumed here, so the average ambipolar conductivity is set equal to the ionic conductivity. Note that the estimate is only intended to be an order of magnitude due to the limited data available.

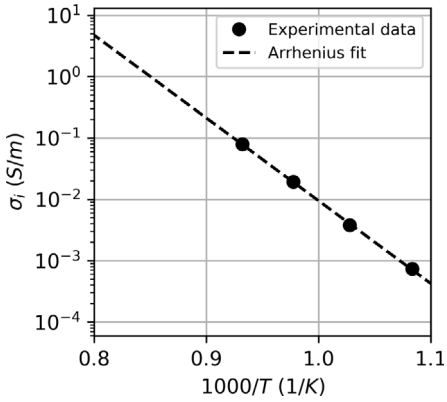

Fig. B.8. Extrapolation of the experimentally determined ionic conductivity of LCF from Bidrawn et al. [37].

References

[1] E. Shelepova, A. Vedyagin, V. Sadykov, N. Mezentseva, Y. Fedorova, O. Smorygo, O. Klenov, I. Mishakov, Theoretical and experimental study of methane partial oxidation to syngas in catalytic membrane reactor with asymmetric oxygen-permeable membrane, Catal. Today 268 (2016) 103–110, http://dx.doi.org/10.1016/j.cattod.2016.01.005.

[2] M.A. Nemitallah, M.A. Habib, S.A. Salaudeen, I. Mansir, Hydrogen production, oxygen separation and syngas oxy-combustion inside a water splitting membrane reactor, Renew. Energy 113 (2017) 221–234, http://dx.doi.org/10.1016/j.renene.2017.05.086.

[3] M.A. Nemitallah, Characteristics of oxygen permeation and partial oxidation of methane in a catalytic membrane reactor for syngas production, Energy Fuels 34 (6) (2020) 7522–7532, http://dx.doi.org/10.1021/acs.energyfuels.0c00630.

[4] T. Zhao, C. Chen, H. Ye, CFD simulation of hydrogen generation and methane combustion inside a water splitting membrane reactor, Energies 14 (21) (2021) 7175, http://dx.doi.org/10.3390/en14217175.

[5] F.T. Akin, J.Y.S. Lin, Oxygen permeation through oxygen ionic or mixed-conducting ceramic membranes with chemical reactions, J. Membr. Sci. 231 (1) (2004) 133–146, http://dx.doi.org/10.1016/j.memsci.2003.11.012.

[6] B. Bulfin, Thermodynamic limits of countercurrent reactor systems, with examples in membrane reactors and the ceria redox cycle, Phys. Chem. Chem. Phys. 21 (4) (2019) 2186–2195, http://dx.doi.org/10.1039/C8CP07077F.

[7] S. McAllister, J.-Y. Chen, A.C. Fernandez-Pello, Fundamentals of Combustion Processes, in: Mechanical Engineering Series, Springer, New York, 2011, http://dx.doi.org/10.1007/978-1-4419-7943-8.

[8] J. Zhu, D. Zhang, K.D. King, Reforming of CH4 by partial oxidation: Thermodynamic and kinetic analyses, Fuel 80 (7) (2001) 899–905, http://dx.doi.org/10.1016/S0016-2361(00)00165-4.

[9] J. Solsvik, T. Haug-Warberg, H.A. Jakobsen, Implementation of chemical reaction equilibrium by Gibbs and Helmholtz energies in tubular reactor models: Application to the steam–methane reforming process, Chem. Eng. Sci. 140 (2016) 261–278, http://dx.doi.org/10.1016/j.ces.2015.10.011.

[10] X. Li, J. Grace, P. Watkinson, J. Lim, A. Ergüdenler, Equilibrium modeling of gasification: A free energy minimization approach and its application to a circulating fluidized bed coal gasifier, Fuel 80 (2001) 195–207, http://dx.doi.org/10.1016/S0016-2361(00)00074-0.

[11] A.C.D. Freitas, R. Guirardello, Comparison of several glycerol reforming methods for hydrogen and syngas production using Gibbs energy minimization, Int. J. Hydrogen Energy 39 (31) (2014) 17969–17984, http://dx.doi.org/10.1016/j.ijhydene.2014.03.130.

[12] S. Adhikari, S. Fernando, S.R. Gwaltney, S.D. Filip To, R. Mark Bricka, P.H. Steele, A. Haryanto, A thermodynamic analysis of hydrogen production by steam reforming of glycerol, Int. J. Hydrogen Energy 32 (14) (2007) 2875–2880, http://dx.doi.org/10.1016/j.ijhydene.2007.03.023.

[13] A. Gambarotta, M. Morini, A. Zubani, A non-stoichiometric equilibrium model for the simulation of the biomass gasification process, Appl. Energy 227 (2018) 119–127, http://dx.doi.org/10.1016/j.apenergy.2017.07.135.

[14] Z. Rui, M. Anderson, Y. Lin, Y. Li, Modeling and analysis of carbon dioxide permeation through ceramic-carbonate dual-phase membranes, J. Membr. Sci. 345 (1–2) (2009) 110–118, http://dx.doi.org/10.1016/j.memsci.2009.08.034.

[15] J.M. Smith, Introduction to chemical engineering thermodynamics, J. Chem. Educ. 27 (10) (1950) 584, http://dx.doi.org/10.1021/ed027p584.3.

[16] W.J. Rankin, Chemical Thermodynamics: Theory and Applications, CRC Press, Boca Raton, 2019, http://dx.doi.org/10.1201/9780429277252.

[17] G. Chen, A. Feldhoff, A. Weidenkaff, C. Li, S. Liu, X. Zhu, J. Sunarso, K. Huang, X.-Y. Wu, A.F. Ghoniem, W. Yang, J. Xue, H. Wang, Z. Shao, J.H. Duffy, K.S. Brinkman, X. Tan, Y. Zhang, H. Jiang, R. Costa, K.A. Friedrich, R. Kriegel, Roadmap for sustainable mixed ionic-electronic conducting membranes, Adv. Funct. Mater. 32 (6) (2022) 2105702, http://dx.doi.org/10.1002/adfm.202105702.

[18] H.J.M. Bouwmeester, H. Kruidhof, A.J. Burggraaf, Importance of the surface exchange kinetics as rate limiting step in oxygen permeation through mixed-conducting oxides, Solid State Ion. 72 (Part 2) (1994) 185–194, http://dx.doi.org/10.1016/0167-2738(94)90145-7.

[19] S.J. Xu, W.J. Thomson, Oxygen permeation rates through ion-conducting perovskite membranes, Chem. Eng. Sci. 54 (17) (1999) 3839–3850, http://dx.doi.org/10.1016/S0009-2509(99)00015-9.

[20] F. Schulze-Küppers, S. Baumann, W. Meulenberg, D. Stöver, H.-P. Buchkremer, Manufacturing and performance of advanced supported Ba0.5Sr0.5Co0.8Fe0.2O3-δ (BSCF) oxygen transport membranes, J. Membr. Sci. 433 (2013) 121–125, http://dx.doi.org/10.1016/j.memsci.2013.01.028.

[21] U. Unije, R. Mücke, P. Niehoff, S. Baumann, R. Vaßen, O. Guillon, Simulation of the effect of the porous support on flux through an asymmetric oxygen transport membrane, J. Membr. Sci. 524 (2017) 334–343, http://dx.doi.org/10.1016/j.memsci.2016.10.037.

[22] K. Wilkner, R. Mücke, S. Baumann, W. Meulenberg, O. Guillon, Sensitivity of material, microstructure and operational parameters on the performance of asymmetric oxygen transport membranes: Guidance from modeling, Membranes 12 (2022) 614, http://dx.doi.org/10.3390/membranes12060614.

[23] D.G. Goodwin, H.K. Moffat, I. Schiegl, R.L. Speth, B.W. Weber, Cantera: An object-oriented software toolkit for chemical kinetics, thermodynamics, and transport processes, 2022, http://dx.doi.org/10.5281/zenodo.6387882.

[24] P. Virtanen, R. Gommers, T.E. Oliphant, M. Haberland, T. Reddy, D. Cournapeau, E. Burovski, P. Peterson, W. Weckesser, J. Bright, S.J. van der Walt, M. Brett, J. Wilson, K.J. Millman, N. Mayorov, A.R.J. Nelson, E. Jones, R. Kern, E. Larson, C.J. Carey, I. Polat, Y. Feng, E.W. Moore, J. VanderPlas, D. Laxalde, J. Perktold, R. Cimrman, I. Henriksen, E.A. Quintero, C.R. Harris, A.M. Archibald, A.H. Ribeiro, F. Pedregosa, P. van Mulbregt, SciPy 1.0: Fundamental algorithms for scientific computing in Python, Nature Methods 17 (3) (2020) 261–272, http://dx.doi.org/10.1038/s41592-019-0686-2.

[25] G.P. Smith, D.M. Golden, M. Frenklach, N.W. Moriarty, B. Eiteneer, M. Goldenberg, C.T. Bowman, R.K. Hanson, S. Song, W.C.J. Gardiner, V.V. Lissianski, Z. Qin, Gri-Mech 3.0.

[26] B. McBride, M. Zehe, S. Gordon, NASA glenn coefficients for calculating thermodynamic properties of individual species, 2002.

[27] L. Cai, S. Hu, Z. Cao, H. Li, X. Zhu, W. Yang, Dual-phase membrane reactor for hydrogen separation with high tolerance to CO2 and H2S impurities, AIChE J. 65 (2018) http://dx.doi.org/10.1002/aic.16491.

[28] S. Zhang, T. Li, B. Wang, Z. Zhou, X. Meng, N. Yang, X. Zhu, S. Liu, Coupling water splitting and partial oxidation of methane (POM) in Ag modified La0.8Ca0.2Fe0.94O3-δ hollow fiber membrane reactors for co-production of H2 and syngas, J. Membr. Sci. 659 (2022) 120772, http://dx.doi.org/10.1016/j.memsci.2022.120772.

[29] V.L. Kozhevnikov, I.A. Leonidov, M.V. Patrakeev, A.A. Markov, Y.N. Blinovskov, Evaluation of La0.5Sr0.5FeO3-δ membrane reactors for partial oxidation of methane, J. Solid State Electrochem. 13 (3) (2009) 391–395, http://dx.doi.org/10.1007/s10008-008-0572-9.

[30] W. Li, X. Zhu, Z. Cao, W. Wang, W. Yang, Mixed ionic-electronic conducting (MIEC) membranes for hydrogen production from water splitting, Int. J. Hydrogen Energy 40 (8) (2015) 3452–3461, http://dx.doi.org/10.1016/j.ijhydene.2014.10.080.

[31] T. Liu, C. Snyder, G. Veser, Catalytic partial oxidation of methane: Is a distinction between direct and indirect pathways meaningful? Ind. Eng. Chem. Res. 46 (26) (2007) 9045–9052, http://dx.doi.org/10.1021/ie070062z.

[32] A.H. Elbadawi, L. Ge, Z. Li, S. Liu, S. Wang, Z. Zhu, Catalytic partial oxidation of methane to syngas: Review of perovskite catalysts and membrane reactors, Catal. Rev. 63 (1) (2021) 1–67, http://dx.doi.org/10.1080/01614940.2020.1743420.

[33] A.P. York, T. Xiao, M.L. Green, Brief overview of the partial oxidation of methane to synthesis gas, Top. Catalysis 22 (3) (2003) 345–358, http://dx.doi.org/10.1023/A:1023552709642.

[34] P.V. Hendriksen, P.H. Larsen, M. Mogensen, F.W. Poulsen, K. Wiik, Prospects and problems of dense oxygen permeable membranes, Catal. Today 56 (1) (2000) 283–295, http://dx.doi.org/10.1016/S0920-5861(99)00286-2.

[35] H. Jiang, H. Wang, S. Werth, T. Schiestel, J. Caro, Simultaneous production of hydrogen and synthesis gas by combining water splitting with partial oxidation of methane in a hollow-fiber membrane reactor, Angew. Chem. 120 (48) (2008) 9481–9484, http://dx.doi.org/10.1002/ange.200803899.

[36] M.V. Patrakeev, J.A. Bahteeva, E.B. Mitberg, I.A. Leonidov, V.L. Kozhevnikov, K.R. Poeppelmeier, Electron/hole and ion transport in La1-xSrxFeO3-δ, J. Solid State Chem. 172 (1) (2003) 219–231, http://dx.doi.org/10.1016/S0022-4596(03)00040-9.

[37] F. Bidrawn, S. Lee, J.M. Vohs, R.J. Gorte, The effect of Ca, Sr, and Ba doping on the ionic conductivity and cathode performance of LaFeO3, J. Electrochem. Soc. 155 (7) (2008) B660, http://dx.doi.org/10.1149/1.2907431.

[38] J.M. Serra, J. Garcia-Fayos, S. Baumann, F. Schulze-Küppers, W.A. Meulenberg, Oxygen permeation through tape-cast asymmetric all-La0.6Sr0.4Co0.2Fe0.8O3-δ membranes, J. Membr. Sci. 447 (2013) 297–305, http://dx.doi.org/10.1016/j.memsci.2013.07.030.